frontiers in
IN CELLULAR NEUROSCIENCE

Selective modulation of cellular voltage dependent calcium channels by hyperbaric pressure - a suggested HPNS partial mechanism

Ben Aviner, Merav Mor_Aviner, Shiri Levy, Gideon Gradwohl and Yoram Grossman

Journal Name:	Frontiers in Cellular Neuroscience
ISSN:	1662-5102
Article type:	Original Research Article
First received on:	09 Sep 2013
Frontiers website link:	www.frontiersin.org

Selective modulation of cellular voltage dependent calcium channels by hyperbaric pressure - a suggested HPNS partial mechanism.

Abstract

Professional deep sea divers experience motor and cognitive impairment, known as High Pressure Neurological Syndrome (HPNS), when exposed to pressures of 100 msw (1.1MPa) and above, considered to be the result of synaptic transmission alteration. Previous studies have indicated modulation of presynaptic Ca^{2+} currents at high pressure. We directly measured for the first time pressure effects on the currents of voltage dependent Ca^{2+} channels (VDCCs) expressed in *Xenopus* oocytes. Pressure selectivity augmented the current in $Ca_V1.2$ and depressed it in $Ca_V3.2$ channels. Pressure application also affected the channels' kinetics, such as τ_{Rise}, τ_{Decay}. Pressure modulation of VDCCs seems to play an important role in generation of HPNS signs and symptoms.

Introduction

HPNS: Unlike chemical factors, pressure acts instantaneously and throughout the organism. Every chemical reaction contributing to the continued existence of the organism is a potential target for pressure effects on biological processes. The major neurological problems associated with hyperbaric environments include N_2 narcosis (inert-gas narcosis), O_2 toxicity, which occurs due to increased oxidative stress (Allen, Demchenko et al. 2009), and HPNS (Halsey 1982; Talpalar and Grossman 2006). By controlling partial-pressures of absorbed tissue gases while under pressure these neurological problems, excluding HPNS, can be alleviated and even eliminated, leading to the notion that HPNS occurs due to effects of pressure *per se* (Abraini 1997; Bennett 1997). Deep sea divers (approximately >100 m), as well as animals exposed to hyperbaric pressure (HP), may experience HPNS, which includes in humans dizziness, nausea, tremors, vision and auditory disturbances, decrements in locomotor activity (Tarasiuk and Grossman 1990; Darbin, Risso et al. 2000) and intellectual performances (Logue, Schmitt et al. 1986; Vaernes, Bergan et al. 1988; Overman, Brauer et al. 1989; Abraini 1997; Steevens, Russell et al. 1999), confusion, changes in EEG & sleep disorders (Rostain, Gardette-Chauffour et al. 1997), myoclonus (Darbin, Risso et al. 2000), convulsions, and loss of conciseness.

Synaptic transmission: Changes in synaptic transmission properties is a possible explanation for this constellation of signs and symptoms (for review see (Daniels and Grossman 2003). Indeed, it has been previously shown that synaptic transmission is suppressed by HP whether in vertebrate CNS synapses (Parmentier, Shrivastav et al. 1981; Schleifstein-Attias, Tarasiuk et al. 1994), squid giant synapse (Parmentier, Shrivastav et al. 1981) or crustacean neuromuscular junction (NMJ) (Campenot 1975; Grossman and Kendig 1990), either in excitatory (Grossman and Kendig 1988; Golan, Moore et al. 1994)or inhibitory (Golan, Moore et al. 1994) synapses. The process of transmitter release from presynaptic terminals is believed to be the same for excitatory and inhibitory synapses; hence it seems acceptable that HP similarly

affects excitation and inhibition. Postsynaptic reduction in receptor sensitivity, observed in glycine receptors (Shelton, Doyle et al. 1993), will exacerbate pressure induced suppression in specific synapses (Daniels and Grossman 2003). Various mechanisms for HP effects on synaptic transmission have been suggested over the past few decades, including modulation of ionotropic receptors activity (Heinemann, Conti et al. 1987; Shelton, Doyle et al. 1993), decreased AP amplitude (Aviner, Gradwohl et al. 2013) and slowed kinetics (Grossman and Kendig 1986; Etzion and Grossman 1999), generally observed depression of neurotransmitter release (Parmentier, Shrivastav et al. 1981; Ashford, MacDonald et al. 1982; Gilman, Colton et al. 1987; Etzion, Mor et al. 2008), decreased vesicle fusion (Ashford, MacDonald et al. 1982; Heinemann, Conti et al. 1987), and the reduction of Ca^{2+} currents (Talpalar and Grossman 2003; Aviner, Gradwohl et al. 2013). HP also causes an increase in synaptic facilitation and tetanic potentiation (Grossman and Kendig 1988), and a decrease in the frequency of spontaneous miniature excitatory postsynaptic potentials (Ashford, MacDonald et al. 1982). The latter phenomena may also suggest that $[Ca^{2+}]_i$ could be involved in manifesting these HP effects. Indeed, it was also found that HP mimics the effects of low $[Ca^{2+}]_o$ (Grossman and Kendig 1990; Etzion, Mor et al. 2008), and in contrast, high $[Ca^{2+}]_o$ can antagonize HP effects (Golan and Grossman 1992; Talpalar, Giugliano et al. 2010; Aviner, Gradwohl et al. 2013). Taken together, we may postulate that one of the major mechanism by which HP suppresses synaptic transmission is a depresion of Ca^{2+} influx into the presynaptic terminal through voltage dependent Ca^{2+} channels (VDCC), which is the natural trigger of this process. Indeed, Grossman and his colleagues have presented an indirect (Grossman and Kendig 1990; Grossman, Colton et al. 1991; Etzion and Grossman 2000) and a semi-direct (Aviner, Gradwohl et al. 2013) evidence for this HP effect on voltage dependent Ca^{2+} currents.

Pressure and voltage dependent Ca^{2+} channels: Various VDCC types exist, characterized by their electrophysiological and pharmacological traits (Ca_V1.1-4, Ca_V2.1-3, Ca_V3.1-3) and comprised of the α_1, $\alpha_2\delta$, β and γ subunits (Meir, Ginsburg et al. 1999; Catterall 2000). The major difference between the channels results from the variation in the α_1 subunit, which holds the ion conducting pore, the voltage sensor, the channel gating section, and the known sites of channel regulation by second messengers, drugs and toxins (Ertel, Campbell et al. 2000). Evidence have accumulated, mostly indirectly, for HP effects on VDCC (Aviner, Gnatek et al. 2010). Pressure inhibited the brief reversal of swimming direction in the *Paramecium,* suggesting that an unclassified Ca^{2+} current, which is associated with the reflex, is impaired (Otter and Salmon 1985). Depolarization dependent Ca^{2+} influx into rat brain synaptosomes was depressed by pressure (Gilman, Kumaroo et al. 1986). Membrane retrieval, another Ca^{2+} dependent process (Vogel, Smith et al. 1999; Wu, McNeil et al. 2009), was also inhibited by pressure (Heidelberger, Zhou et al. 2002).

Analysis of studies on crustacean neuromuscular synapses that examined the relationship between $[Ca^{2+}]_o$, EPSC amplitude and facilitation (Grossman and Kendig 1988; Grossman and Kendig 1990; Golan and Grossman 1992) suggests that pressure is acting to reduce Ca^{2+} influx, rather than to affect intracellular removal of Ca^{2+} or the release process.

The amplitude of slow after-hyperpolarization (sAHP) in rat CA1 was reduced by HP (Southan and Wann 1996). This reduction could be explained by a depression of the SK potassium channel, responsible for the sAHP. But since this channel is activated by the rise of $[Ca^{2+}]_i$ during each AP, it can also be pointing to a reduction in Ca^{2+} influx through VDCCs, not only in the synaptic terminal but also along the axon and possibly in the soma and dendrites as well.

In the frog motor nerve HP significantly suppressed fast Ca^{2+} currents (presumed $Ca_V2.2$), and to a much lesser degree a slow Ca^{2+} currents (presumed Ca_V1 (Aviner, Gradwohl et al. 2013)), suggesting HP selective effect on different types of colocalized VDCCs. The high sensitivity of the $Ca_V2.2$ Ca^{2+} channel to pressure was also suggested in experiments done in the synapse of parallel fibers on Purkinje cells in guinea pig cerebellum (Etzion and Grossman 2000).

On the other hand, in bovine chromaffin cells a slow inactivating Ca^{2+} current was reported insensitive to pressure (Heinemann, Conti et al. 1987), similarly to the Ca^{2+} action potentials , mediated via currents in $Ca_V2.1$ channel , in guinea pig cerebellar Purkinje cells (Etzion and Grossman 1999).

To date, no attempt was made to directly measure isolated Ca^{2+} currents at pressure. The work detailed in this manuscript aims to do so for the first time.

Alteration in the properties of these channels at pressure can significantly influence one's cognition, sensual perception and ability to control posture and muscle activity, in a manifestation which could depict the HPNS.

Methods

Oocytes extraction and cRNA injection: oocytes of *Xenopus laevis* mature female frog were surgically extracted from its ovary and treated with 1.5 mg/ml collagenase for 30-60 minutes in order to remove connecting tissue. Suitable oocytes were sorted out by size, quality and developmental stage (VI), and kept in NDE96 solution containing (in mM): 96 NaCl, 2 KCl, 1 $MgCl_2$, 1 $CaCl_2$, 2.5 sodium pyruvate, 50 µg/ml gentamycine, 5 HEPES, pH 7.5 .

cRNAs of the subunits of L or T type Ca^{2+} channels (LTCC or TTCC, respectively) were synthesized from rabbit cDNA by in-vitro transcription with T7 or SP6 Amplicap High-Yield Message Maker Kit (Epicentre Technologies, Madison, WI). Oocytes were then injected with the specific cRNA mix (2.5 ng) encoding for the pertinent subunits to express LTCC or TTCC were kept in an incubator for 4 days at 18 °C in NDE96 solution. The following subunits were used: $\alpha_{1X}+\beta_{2A}+\alpha_2\delta$, comprising the LTCC $Ca_V1.2$ and $\alpha_{1H}+\alpha_2\delta$, comprising the TTCC $Ca_V3.2$ whose gene code numbers are $\alpha_2\delta$ - M21948, β_2 - X64297, α_{1C} - X15539, and α_{1H} - AF051946.

Electrophysiological recordings: 4 days post injection the oocytes were placed in a specially designed bath, and two electrodes voltage clamp (TEVC) experiments with 10 mV increments and 5-10 sec interval between -70 to 40 mV were performed inside a compression chamber, utilizing an AXOCLAMP 2B amplifier (Molecular Devices, Axon Instruments, Inc, CA, USA), Master-8-cp Pulse Generator (A.M.P.I.) and AxoScope 9.2 software. While in the chamber, each oocyte was continuously perfused with a Ba^{2+} solution containing (in mM) : 40 $Ba(OH)_2$, 50 NaOH, 2 KOH, and 5 HEPES, titrated to pH 7.5 with methanesulfonic acid. Ba^{2+} was used as charge carrier, replacing the Ca^{2+} ions, in order to avoid Ca^{2+} dependent inactivation and the activation of Ca^{2+} activated Cl^- channels (Cl^-_{Ca}), known to be endogenously expressed in oocytes membrane (Miledi and Parker 1984). The channels also have higher conductance to Ba^{2+} (Tsien, Hess et al. 1987), allowing measurement of minute currents that otherwise would have been unnoticed. The solution, saturated with air at atmospheric pressure, was introduced to the chamber by the use of a high pressure pump (Minipump, LDC Analytical Inc, Riviera Beach, FL, USA) at room temperature (24-25°C), at a rate of 1.5-2 ml/min. Temperature was constantly monitored throughout the experiments by the use of a thermistor submerged in the solution in the vicinity of the oocyte groove. Deviation of only ±0.5°C was allowed from the control temperature for later measurements.

Typical recording traces are shown in Fig 1A-B. For the oocytes expressing $Ca_V1.2$ holding potential was -70 mV (Fig 1A). Each depolarizing step duration was 500 ms which was preconditioned by a 100 ms hyperpolarizing step to -80 mV in order to release the VDCC from partial inactivation. The latter was also used to calculate and monitor the oocytes instantaneous input resistance which was accounted for at each recorded trace separately. For the oocytes expressing $Ca_V3.2$ holding potential was -80 mV (fig. 1B) and each depolarizing step duration was 100 ms which was preconditioned by a 150 ms hyperpolarizing step to -90 mV, for similar reasons.

Every series of depolarizing pulses was used to construct an I-V curve and repeated at least three times in order to verify stability of the currents. Recorded traces with voltage fluctuation greater than 2 mV were disregarded. We studied HP effects (examples in fig. 1A-B bottom panels) on I-V curve, maximal currents, activation and inactivation functions, channel's kinetics such as time to peak and time constants (τ), and voltage dependency. Maximal currents were measured as the lowest point of the current curve (Fig 1 inset, left arrow). Inactivation (I/Imax) was measured towards the end of the depolarizing step (Fig 1 inset, right arrow) in comparison to the measured maximal current (as above). A fit was calculated for each decaying section of the current in every recorded trace (fig. 1 inset, blue fit) according to a biexponential equation, defining two time constants for decay:

$$Fit = -A1\exp(-t/\tau_{Decay\ Fast}) - A2\exp(-t/\tau_{Decay\ slow}) + C\ .$$

For the rising phase and the tail currents a single exponential fit was performed (fig. 1 inset, red fits).

Activation volume ($\Delta V^{\ddagger}$) was calculated for time constants of channels activation, inactivation and deactivation under normobaric and hyperbaric conditions, following the known equation: $\Delta V^{\ddagger} = RT(\partial \ln \tau / \partial P)_T$

Truncated K channel: The current measurement using TEVC method was carried out for long duration and under HP conditions. Since it was our first attempt, a verification of the recording stability was needed. AS a first approximation, truncated variant of a *Drosophila* K^+ channel (KCNKØ) missing its carboxy-terminal tail (700 residues) was injected into oocytes (n=4), causing a shift of their normal resting potential from about -40 – -50 mV to approximately -80mV (Zilberberg, Ilan et al. 2000). The membrane potential of these oocytes was then measured for 1-2 h and demonstrated stable resting potential of -80 $\pm$2 mV (not shown) . This result showed that the setup measurements are accurate and do not drift during the experiment.

Ca^{2+}-activated Cl^- channels blocker: In an attempt to clarify whether Ba^{2+} currents measured in the VDCCs, over-expressed in the oocytes membrane, are subjected to artifacts caused by currents via endogenous channels, we have performed a series of experiments in $Ca_V1.2$ channels using 9-Anthracene carboxylic acid (9-AC), a pharmacological blocker of the Cl^-_{Ca} (Boton, Dascal et al. 1989). The use of a Ca^{2+} chelators, e.g. BAPTA or EGTA, was not feasible due to their short time-span effectiveness in relation to the duration of our experiments (see *Results, Time stability of HP effect*). 9-AC was dissolved at 0.2-0.5M in a 1M solution of NaOH. This stock solution was then added to the physiological measurement solution to a final 2-4mM concentration (Boton, Dascal et al. 1989). Titration to pH 7.5 was then done using Methanesulfonic acid.

Helium Compression: After control measurement at 0.1 MPa, compressions steps to 0.5, 1.0, 2.5 and 5.0 MPa were performed by compressed helium. Compression was done manually from a tank through a set of valves into the pressure chamber. Compression rate was approximately 0.25-0.5 MPa / min, and never exceeded 1.0 MPa / min. The use of helium instead of air is due to its inert quality and the need to avoid known nitrogen narcosis and oxygen toxicity related effects (Dean, Mulkey et al. 2003).

Statistical analysis: The full set of parameters was calculated for each recorded trace separately, considering the instantaneous input resistant and leak currents where appropriate, using a self-designed Matlab software program. The data was exported to Microsoft Excel software, by which averaging and binning were performed. Each oocyte was used as its own control, normalized to 0.1 MPa. Where data from more than one oocyte was pooled, binning was performed relative to the voltage generating the maximal current in the I-V curve (V_{Imax}), hence in figures representing these data (1.E-H and 3-9.C-F) the X axis title is 'ΔV' . 'Paired sample t-tests' was used to analyze the significance of the results.

Results

Increased current in $Ca_V1.2$

Generally, HP was expected to suppress currents of VDCCs (see Introduction). Surprisingly, Ba^{2+} currents in $Ca_V1.2$ were significantly increased in oocytes exposed to HP (0.5-5.0 MPa, see example in fig 1C) in a dose dependent manner, throughout the channels' voltage range of activity. Compression to 0.5, 2.5 and 5.0 MPa augmented the maximal currents by 28 ± 10, 58 ± 22 and 70 ± 32%, respectively (fig. 1E, Average ± SEM, $p<0.01$, n=9-17). Decompression back to 0.1 MPa only partially reversed the HP effect, leaving the maximal current 44 ± 19 % increased. Neither the threshold voltage nor the depolarization (V_{Imax}) that generated the largest currents (negative peak in IV curve) were affected.

Normalizing each IV curve under the various pressures to its own maximal (negative) peak (fig. 1G) show almost identical curves, and therefore suggest that the channel's sensitivity to the membrane voltage did not alter as a result of the compression.

Adiabatic temperature change and time stability

Elevation of ambient pressure in these experiments was achieved by gaseous (helium) compression, hence an adiabatic temperature rise has always occurred (typically 0.5-2, but never more than 4 ºC), which was controlled by the rate of compression. Only measurements within 0.5 ºC or less of control temperature were taken under consideration. Therefore, it was needed to wait for the chamber's atmosphere (bath fluid) to cool down (lasting 10-30 min), resulting in 1-2 h long experiments. Fig. 2A shows IV curves in an oocyte expressing $Ca_V1.2$ recorded at 5.0 MPa (post-compression) while cooling back to control temperature (24ºC). As expected, elevated temperature (in addition to the HP) led to an increase in the currents. However, even after the control temperature was regained, the augmented current persisted. This strongly indicates that the temperature fluctuation cannot solely explain the increase in the channel's current and it should reflect a direct effect of HP (as shown in fig. 1C). In order to verify that, and to rule out the possibility that the surprising augmentation of $Ca_V1.2$ current at pressure is only the result of the adiabatic temperature change or a transient HP effect, currents were measured for 1-2 hours post-compression (different experiments n=2, fig. 2B). As can be seen, currents remained stable at HP for long durations after cooling back to control temperature, thus suggesting that the augmentation effect is stable and pressure induced.

Eliminating Ca^{2+}-activated Cl^- channels current contamination

Xenopus oocytes are known to endogenously express the Ca^{2+}-activated Cl^- channels. In order to avoid their activation (leading to inaccurate current measurement) we have used a Ba^{2+} solution with no added Ca^{2+} in our experiments. In order to avoid any current flowing through these channels in the unlikely event of their activation, the solution was also Cl^- free. Performing TEVC experiment on naïve oocytes generated maximal currents in the 10-30 nA range (not shown), considered negligible compared

to 1000 nA and more measured in oocytes expressing the $Ca_V1.2$ channel. Nevertheless, we preformed two sets of experiments aimed to verify that the theoretical Cl^-_{Ca} current does not play a role in the HP related effect, by adding 9-AC (a Ca^{2+}-activated Cl^- channel blocker, see *Methods*) to the solution before or after compression (fig. 2C). Neither adding 9-AC pre-compression alter the HP-induced augmentation of $Ca_V1.2$ current (fig. 2D), nor did 9-AC affected this augmentation when added post-compression, indicating that the HP effect is real.

Ba^{2+} – Ca^{2+} substitution

Since Ca^{2+} was substituted for by Ba^{2+} due to the reasons mention in *Methods*, we wanted to verify that the HP effect is still valid when using the native Ca^{2+} ion. As expected, changing the bath solution to contain Ca^{2+} (using the $Ca_V1.2$ channel) resulted a decrease in the measured current and a faster and stronger inactivation (fig. 2E and 2F black curves). Application of pressure has augmented this current as well (fig. 2F, red curve).

Decreased current in $Ca_V3.2$

Ba^+ currents in $Ca_V3.2$ were significantly decreased at HP (0.5-5.0 MPa) in a dose dependent manner (see example in fig. 1D), in contrast to the findings of $Ca_V1.2$. Preliminary results showed that the HP effect did not change between 2.5 and 5.0 MPa, therefore another pressure step to 1.1 MPa was added in subsequent experiments in order to reveal the HP effect saturation. Neither the threshold voltage nor the V_{Imax} were affected. Compression to 0.5, 1.1, 2.5 and 5.0 MPa depressed the maximal currents by 33 ± 2, 42 ± 6, 34 ± 5 and 27 ± 5 %, respectively (fig. 1F, Average ± SEM, $p<0.01$, n=4-9). Decompression to 0.1 MPa failed to recover the current, which remained depressed by 40 ± 7 %. Normalizing each IV curve under the various pressure conditions to its own maximal (negative) peak (fig. 1H) reveals an increase of the currents in $Ca_V3.2$ at sub-maximal membrane potentials (ΔV -10 mV), but not at V_{Imax} and above. We may hypothesize that this might occur due to a higher probability for transition to the 'open' state of the channel in this voltage range.

Channels conductance

Calculating the channels conductance in relation to the membrane potential show similar results to the general findings in the IV curves (see examples in fig. 3A-B). HP decreased the conductance in the $Ca_V3.2$ channel (fig. 3D) and increased it in the $Ca_V1.2$ channel (fig. 3C). On average, the change from threshold to maximal normalized response occurred within 20 mV depolarization range for $Ca_V3.2$ channel and 30 mV for the $Ca_V1.2$ channel. Normalizing each curve to its own maximal value (fig. 3E-F) reveals in the $Ca_V3.2$ channel the same tendency seen in the normalized IV curve (Fig. 1H) for higher conductance at HP in the ΔV -10 mV membrane potential, whereas the $Ca_V1.2$ channel did not show such trait (fig. 3E). For depolarizations above V_{Imax} only compression to 0.5 MPa caused a consistent small reduction in normalized conductance in both channels.

Currents inactivation

The eminent effect of HP on these channels manifested in the current and conductance parameters has lead us to ask why does pressure changes the total flux through them during supra-threshold depolarizations. A possible explanation could be that the channels' kinetics is affected by pressure. Previous findings have correlated HP to slowed inactivation in Na^+ channel (Henderson and Gilbert 1975; Conti, Fioravanti et al. 1982) and compared the effect of higher pressure to lower temperature (Grossman and Kendig 1984; Grossman and Kendig 1986). We have therefore embarked on testing a few of the channels' kinetic properties. We first examined channels' inactivation, measured as the ratio between remaining fraction of the current at the end of the depolarizing voltage step and its maximal value (I_{end}/I_{max}, see examples in fig. 4A-B). The lack of Ca^{2+} ions in the experimental solution has eliminated the Ca^{2+} dependent inactivation and most likely guaranteed that only the voltage & time dependent inactivation will be measured. To verify this assumption, and in order to serve as a reference, a few experiments were conducted (n=5) using a solution in which the Ba^{2+} was replaced with an equivalent concentration of Ca^{2+} (example in fig. 2E) .As expected, in the presence of Ca^{2+} a stronger (2 folds) and faster (4 folds) inactivation was observed.

For the $Ca_V1.2$ channel inactivation was stronger at V_{Imax} , but was weakened at stronger depolarizations (ΔV 10-40 mV, fig. 4C). Decompression did not relieve the HP effect. For the $Ca_V3.2$ channel, the inactivation was stronger around the threshold voltage (ΔV -20 – -10 mV) at HP, but was weakened at V_{Imax} at lower HP (1.1 MPa).

Normalizing each curve to its own minimal value stresses the tendency for the strongest inactivation to occur in the $Ca_V1.2$ channel at V_{Imax} at HP, whereas at normobaric pressure and post-decompression it occurs at the strongest depolarization, as expected for this VDCC (fig. 4E). For the $Ca_V3.2$ channel although the normalized curves converge at high depolarization, in most supra-threshold membrane potentials inactivation remained stronger at HP (fig. 4F).

Currents time to peak

If the rate of activation of the VDCCs is affected by HP, that may change the time window for the ionic flow through them before the voltage & time dependent inactivation will take place. In case activation is as slow as inactivation, that will affect the I_{max} in each depolarization. We have therefore measured the time passing from the stimulating depolarizing step to the development of I_{max} (time to peak, TTP). Examples can be seen in fig. 5A-B.

For the $Ca_V1.2$ channel the TTP was increased at HP near V_{Imax} (ΔV -10 – 10 mV, fig. 5C). Decompression did not relieve this effect.

For the $Ca_V3.2$ channel TTP was decreased in the range between of ΔV -20 - 0 mV (fig. 5D). An increase of TTP was observed after decompression above V_{Imax}.

Normalizing each TTP curve to its own minimal value (normally achieved at strong depolarization) showed the same tendencies: an increased TTP in the $Ca_V1.2$ channel (fig. 5E) and a decreased TTP in the $Ca_V3.2$ channel (fig. 5F).

Currents τ_{Rise}

A complementary trait for the TTP in regards to the opening of the channel is the time constant of the rising phase of the current, τ_{Rise}. Slower TTP should mean greater τ_{Rise} , and vise versa. Indeed, in the $Ca_V1.2$ HP caused an increase in the τ_{Rise} values at V_{Imax} and 10 mV above (fig. 6A). Greater depolarizations lead to convergence of τ_{Rise} to control values (fig. 6B). Decompression only partially recovered τ_{Rise} , which remained elevated at V_{Imax}. Normalizing each curve to its own minimal value demonstrates a similar rise in τ_{Rise} at V_{Imax} and ΔV 10mV (fig. 6C), which might support the notion that HP interferes with the opening mechanism of this channel, i.e slows its kinetics. $\Delta V^{\ddagger}$ of current activation for $Ca_V1.2$ at V_{Imax} was calculated to be 454 ml/mole at 5.0 MPa.

Unfortunately, relatively large currents measured in the $Ca_V3.2$ channel were accompanied by an artifact during their rising phase, which prevented accurate measurement of their τ_{Rise}.

Currents Fast τ_{Decay}

The changes in inactivation (I_{end}/I_{max}) found in both channels at HP could arise from its effect on their rate of decay, since I_{end} was measured here after a specific time and not under steady state conditions. The analysis revealed fast and slow time constants for the decay (see examples in fig. 7A-B and 8A-B), the first being shortened by stronger depolarizations and the latter being elongated.

For the $Ca_V1.2$ HP caused a decrease in the fast τ_{Decay} ($\tau_{Decay\ fast}$) at V_{Imax} and 10 mV below (fig. 7C). Stronger depolarizations (ΔV 10-40 mV) at HP did not change $\tau_{Decay\ fast}$, but after decompression its values were slightly smaller (ΔV 30-40 mV). At the rest of the depolarizing range decompression has fully recovered $\tau_{Decay\ fast}$. For the $Ca_V3.2$ the ruling trend was a reduction of $\tau_{Decay\ fast}$ at HP, mainly from V_{Imax} and above (fig. 7D), while decompression did not relieve this effect. Normalizing each curve to its own minimal value showed for the $Ca_V1.2$ channel a depression at 2.5 and 5.0 MPa, but not at 0.5 MPa (fig. 7E), while decompression increased the normalized $\tau_{Decay\ fast}$. In the $Ca_V3.2$ channel at ΔV -10 – 0 compression to 1.1 and 5.0 MPa (but not to 0.5 and 2.5 MPa) increased the normalized $\tau_{Decay\ fast}$ (fig. 7F), which remained elevated after decompression in this activity range.

$\Delta V^{\ddagger}$ of fast decay inactivation at V_{Imax} was calculated to be -332 and -55 ml/mole at 5.0 MPa for $Ca_V1.2$ and $Ca_V3.2$, respectively.

Currents slow τ_{Decay}

The slow τ_{Decay} ($\tau_{Decay\ Slow}$) in both channels was increased by stronger depolarizations at 0.1 MPa (fig. 8A-B).

For the $Ca_V1.2$ channel $\tau_{Decay\ Slow}$ does not seem to be sensitive to HP, as no consistent significant difference was found in its values after compression or decompression (fig. 8C). For the $Ca_V3.2$ channel $\tau_{Decay\ Slow}$ was shortened only by strong depolarization (ΔV 30-40 mV) at HP, while decompression eliminated this effect (fig. 8D). The normalized curves of $\tau_{Decay\ Slow}$ for both channels did not reveal a different behavior than that described above (fig. 8E-F).

$\Delta V^{\ddagger}$ of slow decay inactivation at V_{Imax} was calculated to be -32 and 179 ml/mole at 5.0 MPa for $Ca_V1.2$ and $Ca_V3.2$, respectively.

Currents τ_{Tail}

The tail current time constant (τ_{Tail}), representing the kinetics of the channels' deactivation, was shortened by increasing depolarization in the $Ca_V1.2$ channel (see example in fig. 9A). This trend persisted with the application of HP, but at 5.0 MPa τ_{Tail} remained minimal throughout the activity range of the channel (fig. 9B).Strong depolarization (ΔV 10-40 mV) at HP (0.5 & 5.0, but not 2.5 MPa) shortened τ_{Tail}. The normalized curves of τ_{Tail} stress the absence of a significant slope at 5.0 MPa (fig. 9C). $\Delta V^{\ddagger}$ of deactivation for $Ca_V1.2$ at V_{Imax} was calculated to be -432 ml/mole at 5.0 MPa.

Unfortunately, the reciprocal artifact for the one interfering with measuring τ_{Rise} in the $Ca_V3.2$ channel also prevented an accurate measurement of τ_{Tail} .

Discussion

Establishing the methodology

The use of truncated K^+ channel proved the stability of measurements in our setup in these unusually long oocytes experiments, which were necessary due to adiabatic temperature fluctuations. Furthermore, There was no indication to long term (1h) effects of the fluctuating adiabatic temperature on barium currents once control temperature was restored (fig. 2B), suggesting that it cannot account for the much greater pressure-induced changes in maximal currents. Due to the relatively quick response of the preparation (Fig. 2A) and in comparison to previous studies (Grossman and Kendig 1984), it is likely that the time course of recovery from temperature transients is not longer than a few minutes, and therefore at the time of current measurements, when the ambient temperature is within 0.5°c deviation from control value, the membrane does not exhibits properties of a few degrees higher/lower temperature.

Additional support for this assumption arises from experiments in lobster (*Panulirus interruptus*) bifurcating axon, which showed that 10-15 min were sufficient to allow

the responses to recover to the original levels and remain stable (Grossman and Kendig 1986).

In the present experiments, cooling back to control temperature after compression steps lasted 12-15 min, with at least additional 5-6 min required for verifying stability of currents. Thus, the total time of 17-21 min seems pertinent to allow the preparation to 'relax' to its new pressure condition without temperature change interference. However, we can not rule out completely the possibility that transient adiabatic temperature fluctuation contributes to the current change at pressure *per se*. In order to do so, conditions of compression need to allow a constant temperature during pressure changes, i.e. preventing or minimizing adiabatic temperature fluctuations. Only liquid compression can achieve this stipulation to a high degree, but unfortunately cannot be employed in our current setting. Nevertheless, Schmalwasser et al. (1998) (Schmalwasser, Neef et al. 1998) have managed to design and operate a hydrostatic (oil) pressures chamber, in which adiabatic temperature fluctuation in compressions steps of 10 MPa was only 0.5°C or less, and demonstrated a reversible reduction of currents in the *Shaker* potassium channel mutant *Shaker* BD6-46 T449K. These results show that high pressure induced its effects on the channel even when temperature fluctuation was minimized, suggesting that our results were not distorted by the small temperature change.

The use of the 9-AC blocker both in normobaric and HP conditions strongly suggested that the endogenous Cl^-_{Ca} currents are of no significant importance in our experiments (fig. 2C-D). Furthermore, the use of Ba^{2+} as a charge carrier proved to be efficient, as currents were stronger and the Ca^{2+} inactivation was eliminated (fig. 2E) as expected (Lyford, Strege et al. 2002).

Taken together, these control experiments show that the changes demonstrated after compression are indeed pressure related.

The HP induced depression demonstrated in the $Ca_V3.2$ channel further strengthened our findings in the $Ca_V1.2$ channel, ruling out the possibility for it to be a setup related artifact.

Currents activation

Currents' amplitude

We show here, for the first time by direct measurement, that pressure effect can be selective: currents through $Ca_V1.2$ are increased, whereas currents through the $Ca_V3.2$ channel are depressed at HP. It is noteworthy that the $Ca_V3.2$ is more sensitive to pressure changes than the $Ca_V1.2$ channel, as the HP effect saturated already at 1.1 MPa. Furthermore, currents in the $Ca_V1.2$ were partially recovered on return to atmospheric pressure, whereas in the $Ca_V3.2$ currents did not recover. Although the $Ca_V3.2$ channel is found in neuronal somata and much less in the nerve terminals, the findings demonstrate the possibility of selective pressure effects on other types of Ca^{2+} channels (P/Q, N, R) that are believed to be present at the presynaptic nerve

terminals (Uchitel, Protti et al. 1992; Etzion and Grossman 2000). Such a selectivity was already indirectly suggested in our experiments done on frog motor nerve terminals (Aviner, Gradwohl et al. 2013).

The effect on the $Ca_V1.2$ is apparently in contrast to previous reports that suggested reduction in Ca^{2+} influx through $Ca_V2.2$,(Grossman, Colton et al. 1991), a lesser (Etzion and Grossman 2000; Aviner, Gradwohl et al. 2013) or no effect (Heinemann, Conti et al. 1987) in L-type VDCC (Ca_V1) at pressure. The $Ca_V3.2$ current reduction conforms to the above notion. However, in part of the studies (Grossman, Colton et al. 1991; Etzion and Grossman 2000) $Ca_V1.2$ involvement was excluded pharmacologically, while in others it was assumed absent based on information obtained from similar or identical preparations (Robitaille, Adler et al. 1990; French, Lanning et al. 2002). In the chromaffin cells the channels were denoted as Ca_V1 simply due to their similar behavior to these channels in neuronal cells, and have not been characterized pharmacologically. Lastly, the one change observed in Ca^{2+} currents in the bovine chromaffin cells was a slight increase at 40 MPa, which might support our finding of augmentation of currents in the $Ca_V1.2$ (probably a different isoform) at lower pressure. Thus the HP induced increase of current in $Ca_V1.2$ could be specific and excludes other types of channel of the same family (Ca_V1).

The augmentation of the currents in $Ca_V1.2$ channel at HP demonstrated here is reminiscent of another member of this protein superfamily behavior, the K^+ channels. The non-inactivating 'delayed rectifier' K^+ channels pass greater steady-state currents at pressure in invertebrates such as squid (Henderson and Gilbert 1975; Shrivastav BB 1981; Conti, Fioravanti et al. 1982) , snail (Harper, Macdonald et al. 1981) and lobster (Grossman and Kendig 1984). Enhanced K^+ currents at pressure were also proposed as the basis for the firing patterns of Ca^{2+} action potentials in guinea pig Purkinje cells (Etzion and Grossman 1999), and for slowing of the sinus-node pacemaker activity in various mammalian hearts (Ornhagen and Hogan 1977). On the other hand, the reduction of currents in the $Ca_V3.2$ shown here is in agreement with other experiments concerned with an inactivating type of the K^+ channel, demonstrating a depression of currents at pressure in snail (Harper, Macdonald et al. 1981) and in mouse *Shaker* B K^+ channels expressed in *Xenopus* oocytes (Meyer and Heinemann 1997; Schmalwasser, Neef et al. 1998).

Previous studies in our laboratory in rat dentate gyrus corticohippocampal slices suggested that high pressure increases the transfer function between synaptic inputs and somatic spike generation by granule cells, despite the observed reduction of single field excitatory post synaptic potential (fEPSP) amplitude and slope by nearly 50% (Talpalar and Grossman 2004). This suggests that high pressure depresses synaptic activity while increasing excitability in the neuronal dendrites but not in the axons. The $Ca_V1.2$ channels that were studied here are known to be present in the cell bodies and proximal dendrites of neurons in the dentate gyrus (Hell, Westenbroek et al. 1993). It is suggested that pressure-potentiated $Ca_V1.2$ currents in the dendrite may boost subthreshold synaptic potentials to generate action potentials. Such a dendritic hyperexcitability could explain the increased transfer function and is a good

example for another way through which pressure selective effects on VDCC might impact neuronal networks, other than synaptic transmission.

It is interesting to note that the $Ca_V1.2$ is also expressed in the cardiac muscle, and the $Ca_V3.2$ in the cardiac Purkinje fibers. Both changes in the maximal current amplitude described here correlate with previous findings: an increase in the contractility force of isolated rat hearts (Ornhagen and Sigurdsson 1981; Gennser and Ornhagen 1989) and a decrease in the contraction pace in rat (Gennser and Ornhagen 1989) and humans (Linnarsson, Ostlund et al. 1999; Kurita, Nagayoshi et al. 2002).

A positive ionotropic pressure effect at steady-state that was reported for skeletal and cardiac muscles was previously explained by increase of cytosolic Ca^{2+} that may occur due to inhibition of Ca^{2+} removal from the cytosol, either into cellular or extracellular compartments (Daniels and Grossman 2003). Our study may offer a different or additional mechanism for these changes in inotropy.

The augmented $Ca_V1.2$ currents may increase neuronal dendritic excitability and therefore contribute to the generation of HPNS. The contribution to HPNS of the reduction of $Ca_V3.2$ currents is less obvious. These low threshold activated channels are involved especially in generating bursting behavior and rhythmic activity in pace-maker neurons in the reticular thalamic nucleus, thalamus, striatum and cortex, where they are involved in controlling sleep, awareness, executive function, movement planning and modulation and sensory inputs, respectively. We may speculate that the current reduction will slow this activity and impair these neuronal 'clocks' function. This may interfere with time processing, coincidence detection as well as motor and sensory functions in a manner similar to HPNS signs and symptoms. A slower rhythmus at HP was found in humans, where EEG waves shifted from α to θ patterns (Rostain, Gardette-Chauffour et al. 1997). The same study also demonstrated sleep disturbances which were more prominent during the beginning of the compression, subsided later and abolished at decompression, suggesting both transient and reversible HP effect, similarly to the results shown in our experiments.

It is worth noticing that at our hand pressure effect on $Ca_V3.2$ is saturating at about 1.1 MPa. This is well correlated with the pressure experienced by professional divers in the depth of seawater in which they begin to complain of the HPNS signs and symptoms. Therefore, this might be an indication that the $Ca_V3.2$ is also involved in the underlying mechanism of this phenomenon.

It is postulated that the mild symptoms observed at lower pressures such as impaired cognitive capabilities and motor dexterity are the consequence of pacemakers mal function as a result of reduction in $Ca_V3.2$ maximal currents.

Channels conductance

Overall, the calculated conductance behavior relative to the membrane potential (fig. 3) is in accordance with the I-V curves described in figure 1. Although generally the HP effect for $Ca_V1.2$ and $Ca_V3.2$ channels is opposite, at ΔV -10 mV both demonstrate an increase of conductance at HP (5.0 MPa, fig. 3C-D). The $Ca_V3.2$ normalized-to-max conductance curve better shows the channels' postulated tendency to shift to an open state at HP in membrane potentials just over the threshold. However, once depolarization is increased the maximal currents and the conductance are depressed by HP. If HP raises the probability to shift to an open state, why would the currents depress? A possible explanation could be a stronger and faster inactivation of the channel at HP throughout the channels' activity range. Indeed, an indication for that can be seen by a decrease in both I_{end}/I_{max} and $\tau_{Decay\ fast}$ at HP (fig. 4D,F and 7D,F, respectively).

The fact that only compression to 0.5 MPa caused a reduction in the normalized-to-max conductance curve above V_{Imax} in both channels (fig. 3E-F) may suggest a transient sensitivity of their 'voltage sensor' to HP.

Currents TTP and τ_{Rise}

Both TTP and τ_{Rise} have elongated at HP for the $Ca_V1.2$ channel, strongly suggesting a slower activation (fig. 5C and 6C, respectively). A similar HP effect was reported in previous studies on VDCCs in guinea pig single cerebellar Purkinje cells (probably $Ca_V2.1$) (Etzion and Grossman 1999) and frog motor nerve (possibly $Ca_V2.2$) (Aviner, Gradwohl et al. 2013). The velocity of an action potential (AP) was also reduced at HP after a transient increase (Grossman and Kendig 1986).

On the other hand TTP was shortened in a narrow voltage range (-20 mV up to V_{Imax}) in the $Ca_V3.2$ (fig. 5D), suggesting a faster activation of the channel at HP. Nevertheless, shortening of TTP may also point out to a faster inactivation process, which will make the maximal current to appear earlier. This indeed was found in the $Ca_V3.2$, where $\tau_{Decay\ Fast}$ has shortened at HP (fig. 7D). Unfortunately the inability to measure τ_{Rise} for $Ca_V3.2$ in this case prevents distinguishing between the two options. However, the opposite HP effect on TTP, conductance and maximal currents for these channels, together with the fact that $\tau_{Decay\ Fast}$ was not significantly elongated for the $Ca_V1.2$ at HP (fig. 7C) although TTP was increased, may indicate that for the $Ca_V3.2$ τ_{Rise} may be shortened at HP.

Currents inactivation

As expected for a fast inactivating channel, the $Ca_V3.2$ shows a lower value of I_{end}/I_{max} (stronger inactivation) than the $Ca_V1.2$ for any given membrane potential (fig. 4A-D). At V_{Imax} the I_{end}/I_{max} value has decreased for the $Ca_V1.2$ at HP, and the same happened for the $Ca_V3.2$ at ΔV -10 – -20 mV. This correlates well with smaller τ_{Decay}

$_{Fast}$ (faster inactivation) in both channels in this voltage range at HP (fig. 7C-D). On the other hand, stronger depolarization (ΔV 10-40 mV) at HP has lead to weaker inactivation in the $Ca_V1.2$, but not in the $Ca_V3.2$ channel (fig. 4C-D). These findings are not supported by the measured $\tau_{Decay\ Fast}$ in both channels in the same voltage range: it was not changed in the $Ca_V1.2$ and it was still reduced in the $Ca_V3.2$. For the latter it seems that since the inactivation has managed to reach its maximal values at the end of the 100 ms time window (end of depolarizing step), the faster $\tau_{Decay\ Fast}$ at HP has only facilitated the already strong inactivation and did not change its values. For the $Ca_V1.2$ channel the $\tau_{Decay\ Fast}$ averages are generally higher at HP for ΔV 10 and above, although not statistically significant, but probably enough to weaken the measured inactivation. A slower inactivation at HP was also reported in Na^+ channel in bovine chromaffin cells (Heinemann, Conti et al. 1987), but not in the *Helix* snail (Harper, Macdonald et al. 1981).

The flatter normalized-to-minimum curve of inactivation in $Ca_V1.2$ at 0.1 MPa relative to HP curves (fig. 4E) and the linear behavior of $\tau_{Decay\ Fast}$ at 0.1 MPa & after decompression as opposed to the behavior at HP (fig. 7C) both suggest that the molecular mechanism controlling the voltage dependent inactivation is affected by HP.

Notwithstanding, no significant changes were observed in the $\tau_{Decay\ Slow}$ at HP in both channels, supporting the concept of different mechanisms for the fast and slow inactivation (Hering, Berjukow et al. 2000; Sokolov, Weiss et al. 2000), which can also react differently to external treatment (Livneh, Cohen et al. 2006). It was also demonstrated that the molecular structures responsible for these two types of inactivation are differently located in the VDCCs protein (Berjukow, Gapp et al. 1999) and that the fast inactivation may act similarly to the 'ball and chain' mechanism in K^+ channel (Cens, Restituito et al. 1999), while the slow inactivation seems to be at least partially dependent on the interaction between α_1 and β subunits (Sokolov, Weiss et al. 2000). We suggest that the selective HP effect between the two channels inactivation (I_{end}/I_{max} and τ_{Decay}) may arise from different conformational changes at HP, resulting from a different basic spatial organization of the channels, specifically of their inactivation controlling regions.

Currents deactivation

Currents τ_{Tail}

Compression to 0.5 and 5.0 MPa, but not 2.5 MPa, has shortened τ_{Tail} for $Ca_V1.2$, implying a faster deactivation of the channel at HP (fig. 9B). The lack of consistency in the HP effect on τ_{Tail} may suggest a transient effect caused by the initial compression (0.5 MPa) on one hand, and the inability of the deactivating mechanism to compensate for the higher HP (5.0 MPa).

The normalized curves show that in the $Ca_V1.2$ the reduction of τ_{Tail} has saturated at V_{Imax} at normobaric and hyperbaric pressure (fig. 9C). However, at 5.0 MPa

saturation was achieved already at ΔV -10 mV, which may indicate that the closure of the channel is facilitated by high HP.

Summary

HP affected the behavior of both $Ca_V1.2$ and $Ca_V3.2$, whether throughout their membrane potential activity range (maximal current, conductance, τ_{Tail} at 5.0 MPa), or just at a confined voltage range (τ_{Rise}, TTP, inactivation, $\tau_{Decay\ Fast}$). The HP effect on the two channels was generally opposite (maximal currents, conductance, TTP), but some kinetic traits shared the same HP-induced tendencies (inactivation at V_{Imax}, $\tau_{Decay\ Fast}$). Some of the effects may indicate a transient nature (conductance and partially τ_{Tail}), while other suggested that the HP effect can be reversible (mostly for $Ca_V1.2$; $\tau_{Decay\ Fast}$, τ_{Tail}, and partially also maximal current and τ_{Rise}). A summary of the major HP-induced findings is given in table 1.

	I_{max}	Conductance	Inactivation	TTP	τ_{Rise}	$\tau_{Decay\ Fast}$	$\tau_{Decay\ Slow}$	τ_{Tail}
$Ca_V1.2$	↑	↑	↑ (↓)	↑	↑	↓ (=)	=	↓
$Ca_V3.2$	↓	↓	↑(=)	↓	N.A.	↓	= (↓)	N.A.

Table 1. General qualitative effect of HP found in our study on channel characteristics. ↑- increase, ↓- decrease, =- no change, ( )- stronger depolarization.

General considerations

The effect of HP can be targeted either at the channel (and its subunits), or at any external modulator. Some of the characteristics examined in this study exhibited sensitivity (sometimes opposite) to HP that was also dependent on the membrane potential, suggesting the HP affects the channel itself. More specifically, HP may target the channels' 'voltage sensor' and thus affects voltage dependent mechanisms of activation, inactivation and deactivation.

Several studies have demonstrated that replacing a section within a subunit (Tang, Yatani et al. 1993; Zhang, Ellinor et al. 1994) or even a single amino acid (Bourinet, Soong et al. 1999; Hans, Urrutia et al. 1999) can dramatically change its reaction to depolarization. Furthermore, it was suggested that these changes are caused by different spatial organization of the subunits, influencing their interactions (Hering, Berjukow et al. 2000).

Similarly, the HP-induced effects demonstrated in this study may indicate that the conformational changes involved in the channels' activity are facilitated (e.g. activation in the $Ca_V1.2$, fast inactivation in the $Ca_V3.2$) or opposed (e.g. activation in the $Ca_V3.2$, rate of activation in the $Ca_V1.2$) by an elevated ambient pressure. Indeed,

this notion is supported by the calculated activation volumes corresponding to these processes, probably affecting the total ionic flux through the channels at HP. Furthermore, even the basic (i.e. not activated) spatial organization of the subunits and their interactions may be altered by the HP application (e.g. a segment within S4 transmembrane region, holding the positively charged amino acids sequence that serve as a voltage sensor), thus leading to HP sensitivity shown here. For example, the human and rat glycine receptor affinity to its ligand was reduced at HP (Roberts, Shelton et al. 1996). The reduced activity of this inhibitory mechanism may explain the tendency to hyperexcitability upon exposure to HP (HPNS manifestations). A genetic sequencing of the receptor demonstrated a few amino acid switches between the mammals mentioned above and the *Pilot whale*, one of them in the ligand binding site from the non-polar cysteine (human and rat) to the polar arginine (C41R). This switch may protect the whale from hyperexcitability at HP and provide it the ability to dive to extreme depths.

It can therefore be postulated that performing HP experiments on a specific VDCC with altered subunits or a VDCC chimera might further elucidate what is the HP targeted site. Preliminary results from experiments on the NMDA receptor at HP may suggest that even changes in the extracellular N terminal domain can influence the magnitude and direction of the pressure effect (Mor, Kuttner et al.).

Conclusions

a. HP Modulation of various VDCCs is part of HPNS mechanisms and may explain some of its signs and symptoms.

b. HP effects could be quite selective for the type of channel, various mechanisms underlying the channels' activity, and even specific regions of the protein.

c. HP effects on the channels' kinetics should be extensively studied in order to reveal small functional differences under HP conditions.

d. Our study emphasizes the importance of pressure modulation of the membrane potential 'sensor' which may determine the extent of pressure effects on the channels.

References

Abraini, J. H. (1997). "Inert gas and raised pressure: evidence that motor decrements are due to pressure per se and cognitive decrements due to narcotic action." Pflugers Arch **433**(6): 788-91.

Allen, B. W., I. T. Demchenko, et al. (2009). "Two faces of nitric oxide: implications for cellular mechanisms of oxygen toxicity." J Appl Physiol **106**(2): 662-667.

Ashford, M. L., A. G. MacDonald, et al. (1982). "The effects of hydrostatic pressure on the spontaneous release of transmitter at the frog neuromuscular junction." J. Physiol. **333**(1): 531-543.

Aviner, B., Y. Gnatek, et al. (2010). "Hyperbaric pressure effects on voltage-dependent Ca+2 channels: relevance to HPNS." Undersea Hyperb Med **37**(5): 245-58.
Aviner, B., G. Gradwohl, et al. (2013). "Modulation of presynaptic Ca^{2+} currents in frog motor nerve terminals by high pressure." Eur J Neurosci **38**(5): 2716-29.
Bennett, P. B. (1997). "Inert gas narcosis and high pressure nervous syndrome." Bove and Davis' Diving Medicine(3): 117–130.
Berjukow, S., F. Gapp, et al. (1999). "Sequence Differences between alpha 1C and alpha 1S Ca2+ Channel Subunits Reveal Structural Determinants of a Guarded and Modulated Benzothiazepine Receptor." J. Biol. Chem. **274**(10): 6154-6160.
Boton, R., N. Dascal, et al. (1989). "Two calcium-activated chloride conductances in Xenopus laevis oocytes permeabilized with the ionophore A23187." J. Physiol. **408**(1): 511-534.
Bourinet, E., T. W. Soong, et al. (1999). "Splicing of alpha 1A subunit gene generates phenotypic variants of P- and Q-type calcium channels." Nat Neurosci **2**(5): 407-15.
Campenot, R. B. (1975). "The effects of high hydrostatic pressure on transmission at the crustacean neuromuscular junction." Comp Biochem Physiol B **52**(1): 133-40.
Catterall, W. A. (2000). "Structure and regulation of voltage-gated Ca2+ channels." Annu Rev Cell Dev Biol **16**: 521-55.
Cens, T., S. Restituito, et al. (1999). "Voltage and Calcium Use the Same Molecular Determinants to Inactivate Calcium Channels." J. Biol. Chem. **274**(9): 5483-5490.
Conti, F., R. Fioravanti, et al. (1982). "Pressure dependence of the potassium currents of squid giant axon." J Membr Biol **69**(1): 35-40.
Conti, F., R. Fioravanti, et al. (1982). "Pressure dependence of the sodium currents of squid giant axon." J Membr Biol **69**(1): 23-34.
Daniels, S. and Y. Grossman (2003). "Biological effects of pressure." Bennett and Elliott's Physiology and Medicine of Diving, 5th edition: 265-299.
Darbin, O., J. J. Risso, et al. (2000). "High pressure enhanced NMDA activity in the striatum and the globus pallidus: relationships with myoclonia and locomotor and motor activity in rat." Brain Res **852**(1): 62-7.
Dean, J. B., D. K. Mulkey, et al. (2003). "Neuronal sensitivity to hyperoxia, hypercapnia, and inert gases at hyperbaric pressures." J Appl Physiol **95**(3): 883-909.
Ertel, E. A., K. P. Campbell, et al. (2000). "Nomenclature of voltage-gated calcium channels." Neuron **25**(3): 533-5.
Etzion, Y. and Y. Grossman (1999). "Spontaneous Na+ and Ca2+ spike firing of cerebellar Purkinje neurons at high pressure." Pflugers Arch **437**(2): 276-84.
Etzion, Y. and Y. Grossman (2000). "Pressure-induced depression of synaptic transmission in the cerebellar parallel fibre synapse involves suppression of presynaptic N-type Ca2+ channels." Eur J Neurosci **12**(11): 4007-16.
Etzion, Y., A. Mor, et al. (2008). "Differential modulation of cerebellar climbing fiber and parallel fiber synaptic responses at high pressure." J Appl Physiol: 90853.2008.
French, L. B., C. C. Lanning, et al. (2002). "The localization of two voltage-gated calcium channels in the pyloric network of the lobster stomatogastric ganglion." Neuroscience **112**(1): 217-32.
Gennser, M. and H. C. Ornhagen (1989). "Effects of hydrostatic pressure and inert gases on twitch tension." Undersea Biomed Res **16**(6): 415-26.
Gennser, M. and H. C. Ornhagen (1989). "Effects of hydrostatic pressure, H2, N2, and He, on beating frequency of rat atria." Undersea Biomed Res **16**(2): 153-64.
Gilman, S. C., J. S. Colton, et al. (1987). "Effect of pressure on the release of radioactive glycine and gamma-aminobutyric acid from spinal cord synaptosomes." J Neurochem **49**(5): 1571-8.

Gilman, S. C., K. K. Kumaroo, et al. (1986). "Effects of pressure on uptake and release of calcium by brain synaptosomes." J Appl Physiol **60**(4): 1446-1450.
Golan, H. and Y. Grossman (1992). "Synaptic transmission at high pressure: effects of [Ca2+]o." Comp Biochem Physiol Comp Physiol **103**(1): 113-8.
Golan, H., H. J. Moore, et al. (1994). "Quantal analysis of presynaptic inhibition, low [Ca2+]0, and high pressure interactions at crustacean excitatory synapses." Synapse **18**(4): 328-36.
Grossman, Y., J. S. Colton, et al. (1991). "Interaction of Ca-channel blockers and high pressure at the crustacean neuromuscular junction." Neurosci Lett **125**(1): 53-6.
Grossman, Y. and J. J. Kendig (1984). "Pressure and temperature: time-dependent modulation of membrane properties in a bifurcating axon." J Neurophysiol **52**(4): 693-708.
Grossman, Y. and J. J. Kendig (1986). "Pressure and temperature modulation of conduction in a bifurcating axon." Undersea Biomed Res **13**(1): 45-61.
Grossman, Y. and J. J. Kendig (1988). "Synaptic integrative properties at hyperbaric pressure." J Neurophysiol **60**(4): 1497-1512.
Grossman, Y. and J. J. Kendig (1990). "Evidence for reduced presynaptic Ca2+ entry in a lobster neuromuscular junction at high pressure." J. Physiol. **420**(1): 355-364.
Halsey, M. J. (1982). "Effects of high pressure on the central nervous system." Physiol Rev **62**(4): 1341-1377.
Hans, M., A. Urrutia, et al. (1999). "Structural elements in domain IV that influence biophysical and pharmacological properties of human alpha1A-containing high-voltage-activated calcium channels." Biophys J **76**(3): 1384-400.
Harper, A. A., A. G. Macdonald, et al. (1981). "The action of high hydrostatic pressure on the membrane currents of Helix neurones." J. Physiol. **311**(1): 325-339.
Heidelberger, R., Z.-Y. Zhou, et al. (2002). "Multiple Components of Membrane Retrieval in Synaptic Terminals Revealed by Changes in Hydrostatic Pressure." J Neurophysiol **88**(5): 2509-2517.
Heinemann, S. H., F. Conti, et al. (1987). "Effects of hydrostatic pressure on membrane processes. Sodium channels, calcium channels, and exocytosis." J. Gen. Physiol. **90**(6): 765-778.
Hell, J. W., R. E. Westenbroek, et al. (1993). "Identification and differential subcellular localization of the neuronal class C and class D L-type calcium channel alpha 1 subunits." J. Cell Biol. **123**(4): 949-962.
Henderson, J. V. and D. L. Gilbert (1975). "Slowing of ionic currents in the voltage-clamped squid axon by helium pressure." Nature **258**(5533): 351-2.
Hering, S., S. Berjukow, et al. (2000). "Molecular determinants of inactivation in voltage-gated Ca2+ channels." J. Physiol. **528**(2): 237-249.
Kurita, A., H. Nagayoshi, et al. (2002). "Effects of severe hyperbaric pressure on autonomic nerve functions." Mil Med **167**(11): 934-8.
Linnarsson, D., A. Ostlund, et al. (1999). "Hyperbaric bradycardia and hypoventilation in exercising men: effects of ambient pressure and breathing gas." J Appl Physiol **87**(4): 1428-1432.
Livneh, A., R. Cohen, et al. (2006). "A novel molecular inactivation determinant of voltage-gated CaV1.2 L-type Ca2+ channel." Neuroscience **139**(4): 1275-87.
Logue, P. E., F. A. Schmitt, et al. (1986). "Cognitive and emotional changes during a simulated 686-m deep dive." Undersea Biomed Res **13**(2): 225-35.
Lyford, G. L., P. R. Strege, et al. (2002). "alpha 1C (CaV1.2) L-type calcium channel mediates mechanosensitive calcium regulation." Am J Physiol Cell Physiol **283**(3): C1001-1008.
Meir, A., S. Ginsburg, et al. (1999). "Ion Channels in Presynaptic Nerve Terminals and Control of Transmitter Release." Physiol Rev **79**(3): 1019-1088.

Meyer, R. and S. H. Heinemann (1997). "Temperature and pressure dependence of Shaker K+ channel N- and C-type inactivation." Eur Biophys J **26**(6): 433-45.
Miledi, R. and I. Parker (1984). "Chloride current induced by injection of calcium into Xenopus oocytes." J. Physiol. **357**(1): 173-183.
Mor, A., Y. Y. Kuttner, et al. "Pressure-selective modulation of NMDA receptor subtypes may reflect 3D structural differences." Front Cell Neurosci **6**: 37.
Ornhagen, H. C. and P. M. Hogan (1977). "Hydrostatic pressure and mammalian cardiac-pacemaker function." Undersea Biomed Res **4**(4): 347-58.
Ornhagen, H. C. and S. B. Sigurdsson (1981). "Effects of high hydrostatic pressure on rat atrial muscle." Undersea Biomed Res **8**(2): 113-20.
Otter, T. and E. D. Salmon (1985). "Pressure-induced changes in Ca2+-channel excitability in Paramecium." J. Exp. Biol. **117**(1): 29-43.
Overman, W. H., R. W. Brauer, et al. (1989). "Failure to find residual memory deficits in monkeys after repeated HPNS." Undersea Biomed Res **16**(2): 115-27.
Parmentier, J. L., B. B. Shrivastav, et al. (1981). "Hydrostatic pressure reduces synaptic efficiency by inhibiting transmitter release." Undersea Biomed Res **8**(3): 175-83.
Roberts, R. J., C. J. Shelton, et al. (1996). "Glycine activation of human homomeric alpha 1 glycine receptors is sensitive to pressure in the range of the high pressure nervous syndrome." Neurosci Lett **208**(2): 125-8.
Robitaille, R., E. M. Adler, et al. (1990). "Strategic location of calcium channels at transmitter release sites of frog neuromuscular synapses." Neuron **5**(6): 773-9.
Rostain, J. C., M. C. Gardette-Chauffour, et al. (1997). "EEG and sleep disturbances during dives at 450 msw in helium-nitrogen-oxygen mixture." J Appl Physiol **83**(2): 575-582.
Schleifstein-Attias, D., A. Tarasiuk, et al. (1994). High pressure effects on modulation of mammalian spinal monosynaptic reflex. Rochester, USA, Rochester University Press.
Schmalwasser, H., A. Neef, et al. (1998). "Two-electrode voltage clamp of Xenopus oocytes under high hydrostatic pressure." J Neurosci Methods **81**(1-2): 1-7.
Shelton, C. J., M. G. Doyle, et al. (1993). "The effect of high pressure on glycine- and kainate-sensitive receptor channels expressed in Xenopus oocytes." Proc Biol Sci **254**(1340): 131-7.
Shrivastav BB, P. J., Bennett PB (1981). "A Quantitative description of pressure-induced alterations in ionic channels of the squid giant axon." Seventh Symposium on Underwater Physiology, Undersea Society Inc. **7**: 611-619.
Sokolov, S., R. G. Weiss, et al. (2000). "Modulation of slow inactivation in class A Ca2+ channels by {beta}-subunits." J. Physiol. **527**(3): 445-454.
Southan, A. P. and K. T. Wann (1996). "Effects of high helium pressure on intracellular and field potential responses in the CA1 region of the in vitro rat hippocampus." Eur J Neurosci **8**(12): 2571-81.
Steevens, C. C., K. L. Russell, et al. (1999). "Noise-induced neurologic disturbances in divers exposed to intense water-borne sound: two case reports." Undersea Hyperb Med **26**(4): 261-5.
Talpalar, A. E., M. Giugliano, et al. (2010). "Enduring medial perforant path short-term synaptic depression at high pressure." Front Cell Neurosci **4**: 128.
Talpalar, A. E. and Y. Grossman (2003). "Modulation of Rat Corticohippocampal Synaptic Activity by High Pressure and Extracellular Calcium: Single and Frequency Responses." J Neurophysiol **90**(4): 2106-2114.
Talpalar, A. E. and Y. Grossman (2004). "Enhanced Excitability Compensates for High-Pressure-Induced Depression of Cortical Inputs to the Hippocampus." J Neurophysiol **92**(6): 3309-3319.
Talpalar, A. E. and Y. Grossman (2006). "CNS manifestations of HPNS: revisited." Undersea Hyperb Med **33**(3): 205-10.

Tang, S., A. Yatani, et al. (1993). "Molecular localization of regions in the L-type calcium channel critical for dihydropyridine action." Neuron **11**(6): 1013-21.

Tarasiuk, A. and Y. Grossman (1990). "Pressure-induced tremor-associated activity in ventral roots in isolated spinal cord of newborn rats." Undersea Biomed Res **17**(4): 287-96.

Tsien, R. W., P. Hess, et al. (1987). "Calcium channels: mechanisms of selectivity, permeation, and block." Annu Rev Biophys Biophys Chem **16**: 265-90.

Uchitel, O. D., D. A. Protti, et al. (1992). "P-Type Voltage-Dependent Calcium Channel Mediates Presynaptic Calcium Influx and Transmitter Release in Mammalian Synapses." PNAS **89**(8): 3330-3333.

Vaernes, R. J., T. Bergan, et al. (1988). "HPNS effects among 18 divers during compression to 360 msw on heliox." Undersea Biomed Res **15**(4): 241-55.

Vogel, S. S., R. M. Smith, et al. (1999). "Calcium influx is required for endocytotic membrane retrieval." PNAS **96**(9): 5019-5024.

Wu, X. S., B. D. McNeil, et al. (2009). "Ca(2+) and calmodulin initiate all forms of endocytosis during depolarization at a nerve terminal." Nat Neurosci **12**(8): 1003-10.

Zhang, J. F., P. T. Ellinor, et al. (1994). "Molecular determinants of voltage-dependent inactivation in calcium channels." Nature **372**(6501): 97-100.

Zilberberg, N., N. Ilan, et al. (2000). "Opening and Closing of KcnkO Potassium Leak Channels Is Tightly Regulated." J. Gen. Physiol. **116**(5): 721-734.

Figure 1.TIF

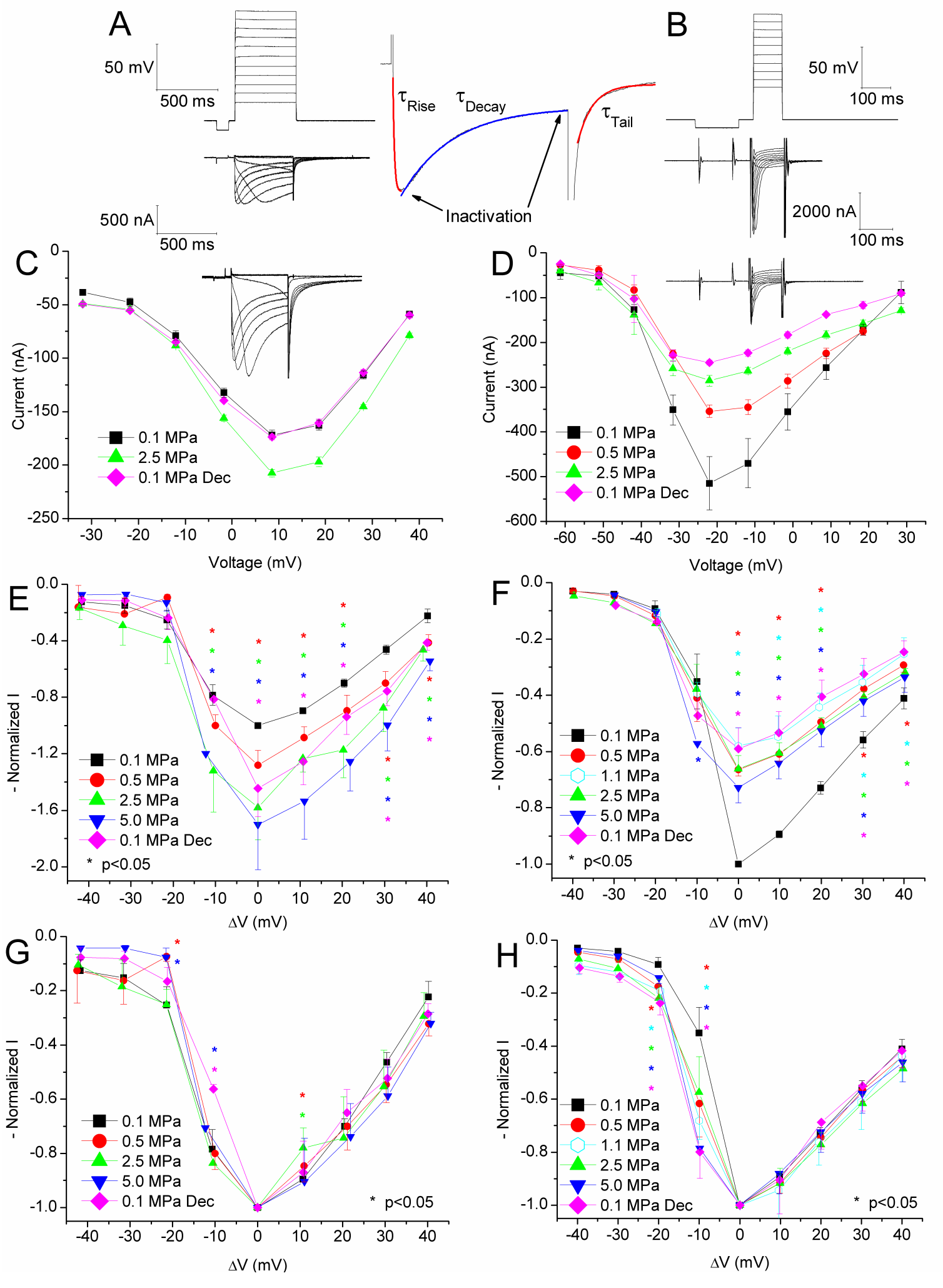
A
50 mV
500 ms
500 nA
500 ms
τRise
τDecay
τTail
Inactivation
B
50 mV
100 ms
2000 nA
100 ms
C
Current (nA)
Voltage (mV)
0.1 MPa
2.5 MPa
0.1 MPa Dec
D
Current (nA)
Voltage (mV)
0.1 MPa
0.5 MPa
2.5 MPa
0.1 MPa Dec
E
- Normalized I
ΔV (mV)
0.1 MPa
0.5 MPa
2.5 MPa
5.0 MPa
0.1 MPa Dec
* p<0.05
F
- Normalized I
ΔV (mV)
0.1 MPa
0.5 MPa
1.1 MPa
2.5 MPa
5.0 MPa
0.1 MPa Dec
* p<0.05
G
- Normalized I
ΔV (mV)
0.1 MPa
0.5 MPa
2.5 MPa
5.0 MPa
0.1 MPa Dec
* p<0.05
H
- Normalized I
ΔV (mV)
0.1 MPa
0.5 MPa
1.1 MPa
2.5 MPa
5.0 MPa
0.1 MPa Dec
* p<0.05

Figure 2.TIF

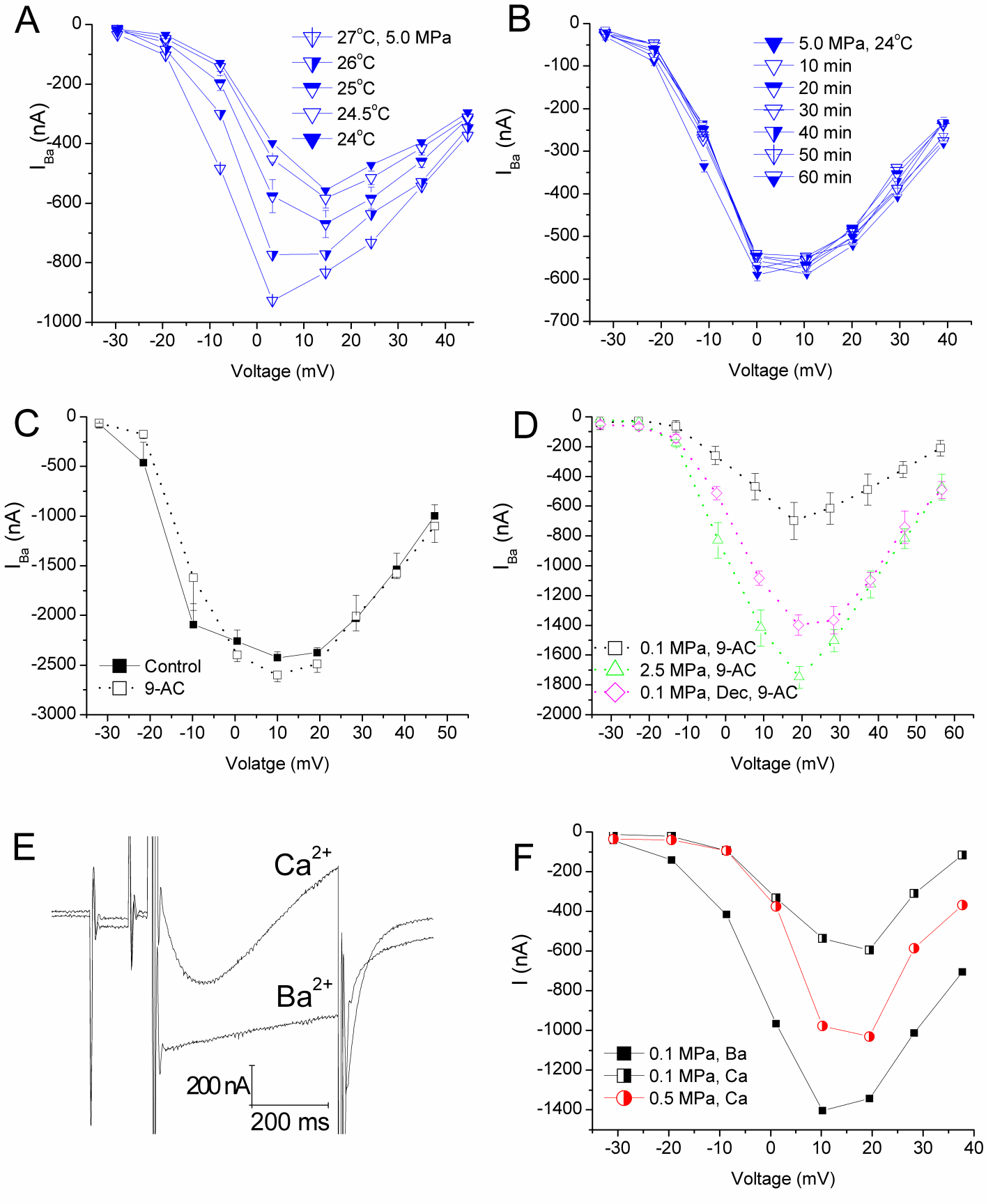
A
27°C, 5.0 MPa
26°C
25°C
24.5°C
24°C
I_Ba (nA)
Voltage (mV)
B
5.0 MPa, 24°C
10 min
20 min
30 min
40 min
50 min
60 min
I_Ba (nA)
Voltage (mV)
C
Control
9-AC
I_Ba (nA)
Volatge (mV)
D
0.1 MPa, 9-AC
2.5 MPa, 9-AC
0.1 MPa, Dec, 9-AC
I_Ba (nA)
Voltage (mV)
E
Ca2+
Ba2+
200 nA
200 ms
F
0.1 MPa, Ba
0.1 MPa, Ca
0.5 MPa, Ca
I (nA)
Voltage (mV)

Figure 3.TIF

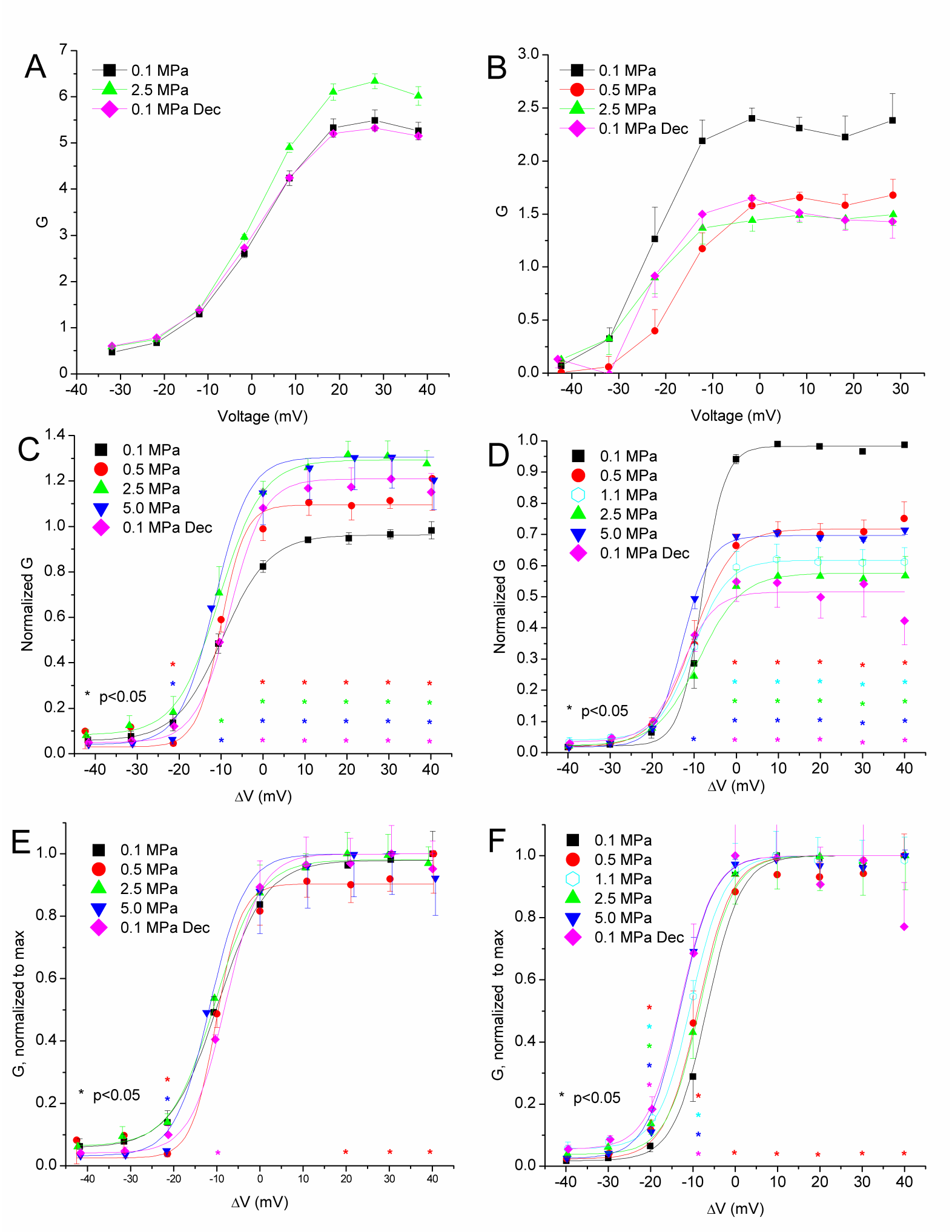
A
0.1 MPa
2.5 MPa
0.1 MPa Dec
G
Voltage (mV)
B
0.1 MPa
0.5 MPa
2.5 MPa
0.1 MPa Dec
G
Voltage (mV)
C
0.1 MPa
0.5 MPa
2.5 MPa
5.0 MPa
0.1 MPa Dec
Normalized G
* p<0.05
ΔV (mV)
D
0.1 MPa
0.5 MPa
1.1 MPa
2.5 MPa
5.0 MPa
0.1 MPa Dec
Normalized G
* p<0.05
ΔV (mV)
E
0.1 MPa
0.5 MPa
2.5 MPa
5.0 MPa
0.1 MPa Dec
G, normalized to max
* p<0.05
ΔV (mV)
F
0.1 MPa
0.5 MPa
1.1 MPa
2.5 MPa
5.0 MPa
0.1 MPa Dec
G, normalized to max
* p<0.05
ΔV (mV)

Figure 4.TIF

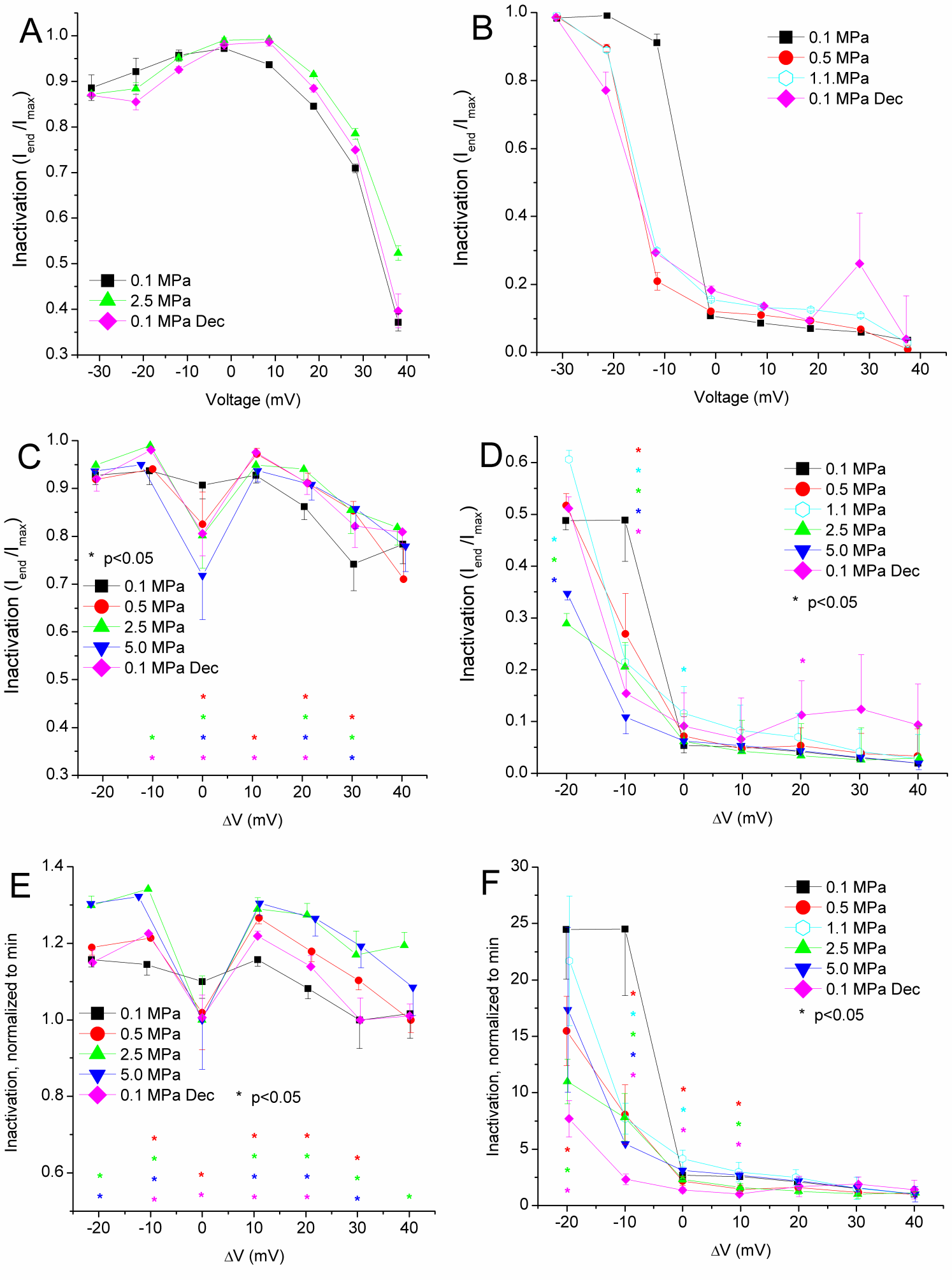
A
Inactivation (I_{end}/I_{max})
Voltage (mV)
0.1 MPa
2.5 MPa
0.1 MPa Dec
B
Inactivation (I_{end}/I_{max})
Voltage (mV)
0.1 MPa
0.5 MPa
1.1.MPa
0.1 MPa Dec
C
Inactivation (I_{end}/I_{max})
ΔV (mV)
* p<0.05
0.1 MPa
0.5 MPa
2.5 MPa
5.0 MPa
0.1 MPa Dec
D
Inactivation (I_{end}/I_{max})
ΔV (mV)
0.1 MPa
0.5 MPa
1.1 MPa
2.5 MPa
5.0 MPa
0.1 MPa Dec
* p<0.05
E
Inactivation, normalized to min
ΔV (mV)
0.1 MPa
0.5 MPa
2.5 MPa
5.0 MPa
0.1 MPa Dec
* p<0.05
F
Inactivation, normalized to min
ΔV (mV)
0.1 MPa
0.5 MPa
1.1 MPa
2.5 MPa
5.0 MPa
0.1 MPa Dec
* p<0.05

Figure 5.TIF

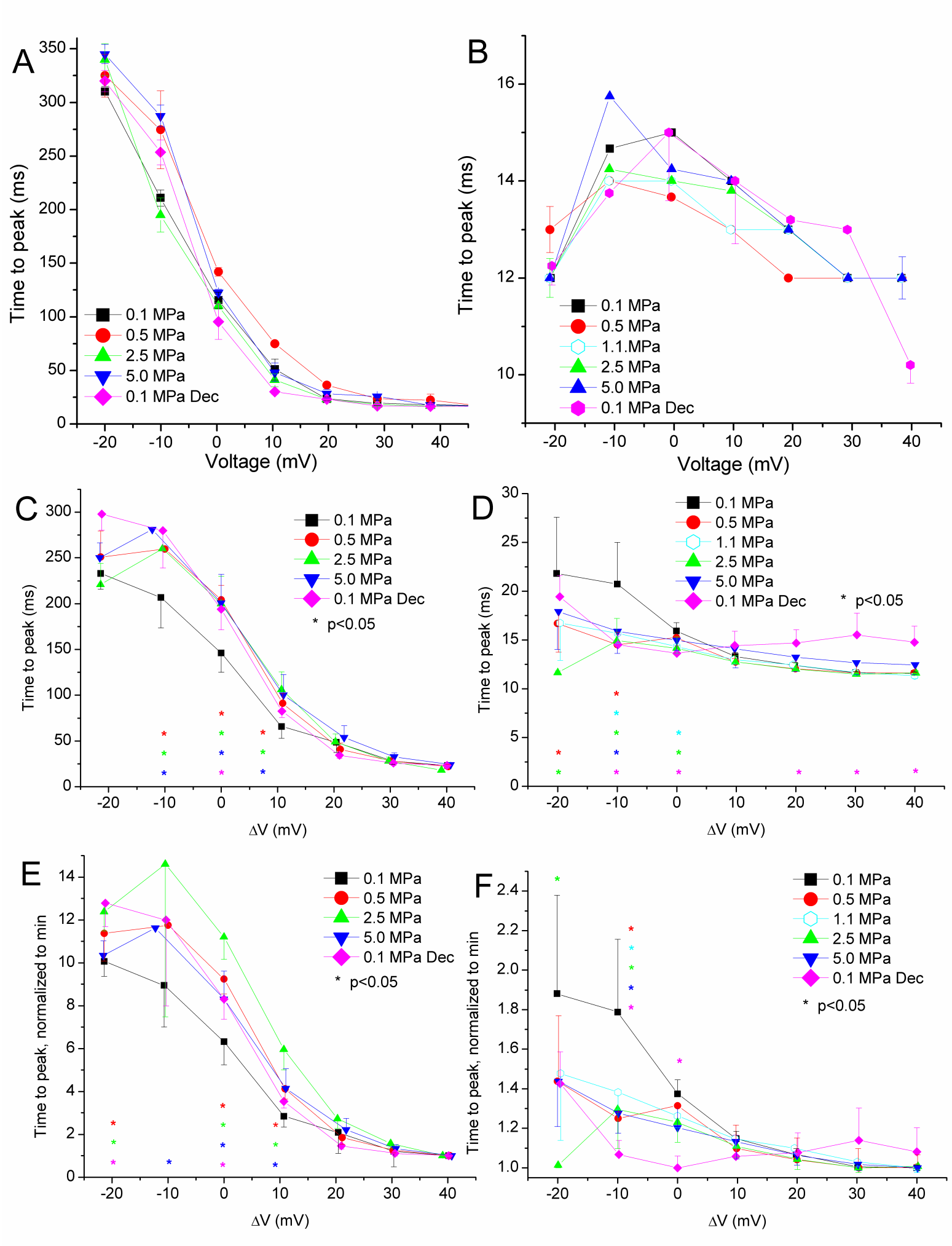
A
Time to peak (ms)
Voltage (mV)
0.1 MPa
0.5 MPa
2.5 MPa
5.0 MPa
0.1 MPa Dec
B
Time to peak (ms)
Voltage (mV)
0.1 MPa
0.5 MPa
1.1.MPa
2.5 MPa
5.0 MPa
0.1 MPa Dec
C
Time to peak (ms)
ΔV (mV)
0.1 MPa
0.5 MPa
2.5 MPa
5.0 MPa
0.1 MPa Dec
* p<0.05
D
Time to peak (ms)
ΔV (mV)
0.1 MPa
0.5 MPa
1.1 MPa
2.5 MPa
5.0 MPa
0.1 MPa Dec
* p<0.05
E
Time to peak, normalized to min
ΔV (mV)
0.1 MPa
0.5 MPa
2.5 MPa
5.0 MPa
0.1 MPa Dec
* p<0.05
F
Time to peak, normalized to min
ΔV (mV)
0.1 MPa
0.5 MPa
1.1 MPa
2.5 MPa
5.0 MPa
0.1 MPa Dec
* p<0.05

Figure 6.TIF

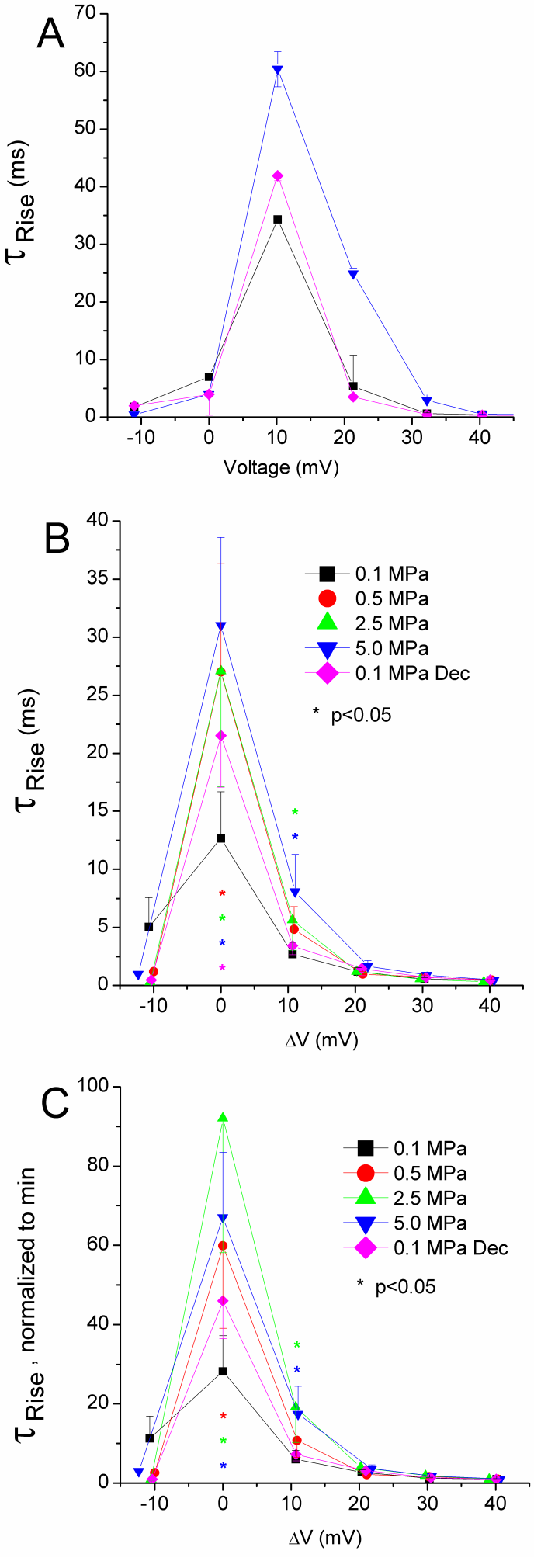
A
τ Rise (ms)
Voltage (mV)
B
τ Rise (ms)
ΔV (mV)
0.1 MPa
0.5 MPa
2.5 MPa
5.0 MPa
0.1 MPa Dec
* p<0.05
C
τ Rise , normalized to min
ΔV (mV)
0.1 MPa
0.5 MPa
2.5 MPa
5.0 MPa
0.1 MPa Dec
* p<0.05

Figure 7.TIF

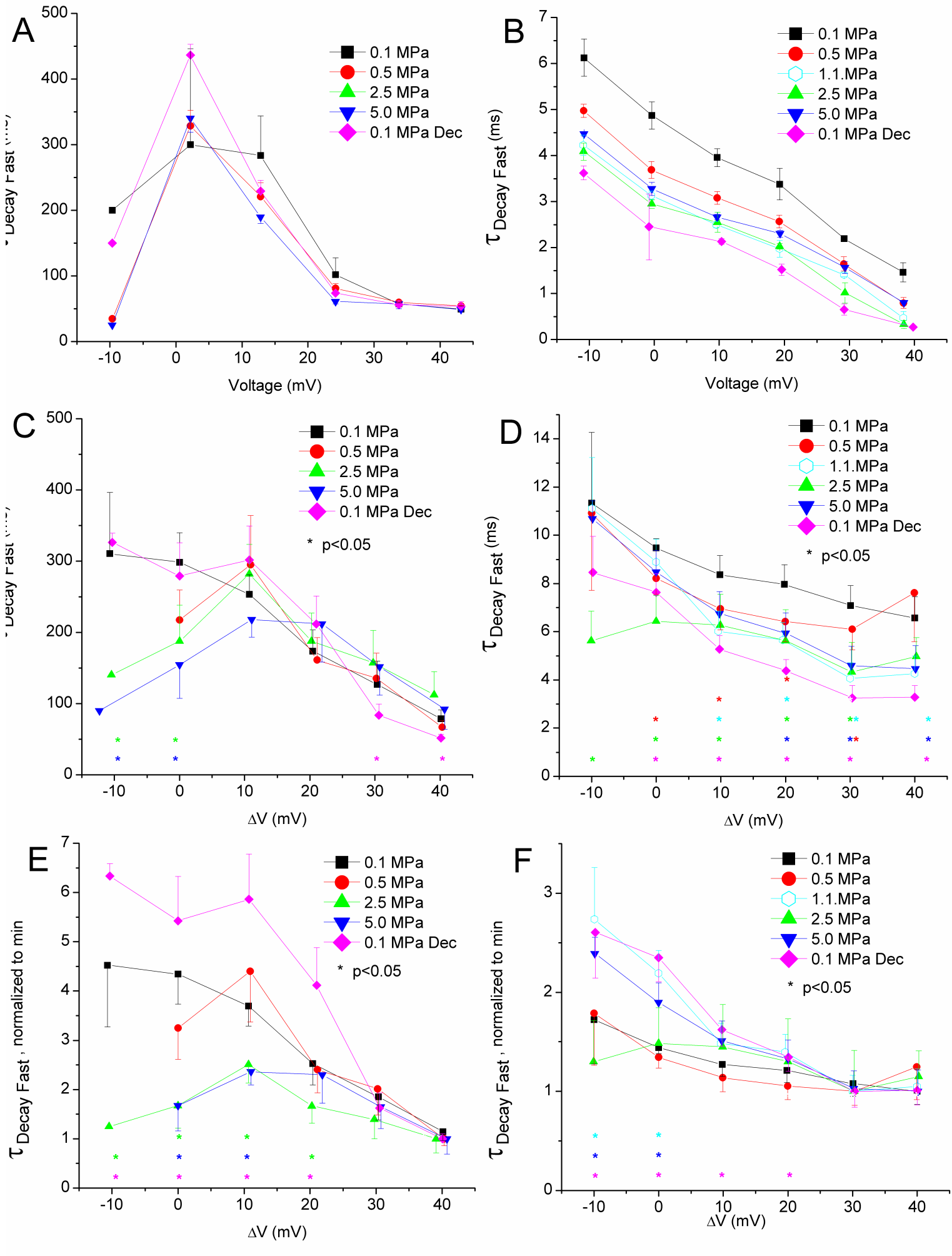
A
B
C
D
E
F
0.1 MPa
0.5 MPa
1.1.MPa
2.5 MPa
5.0 MPa
0.1 MPa Dec
* p<0.05
Voltage (mV)
ΔV (mV)
τ Decay Fast (ms)
τ Decay Fast , normalized to min

Figure 8.TIF

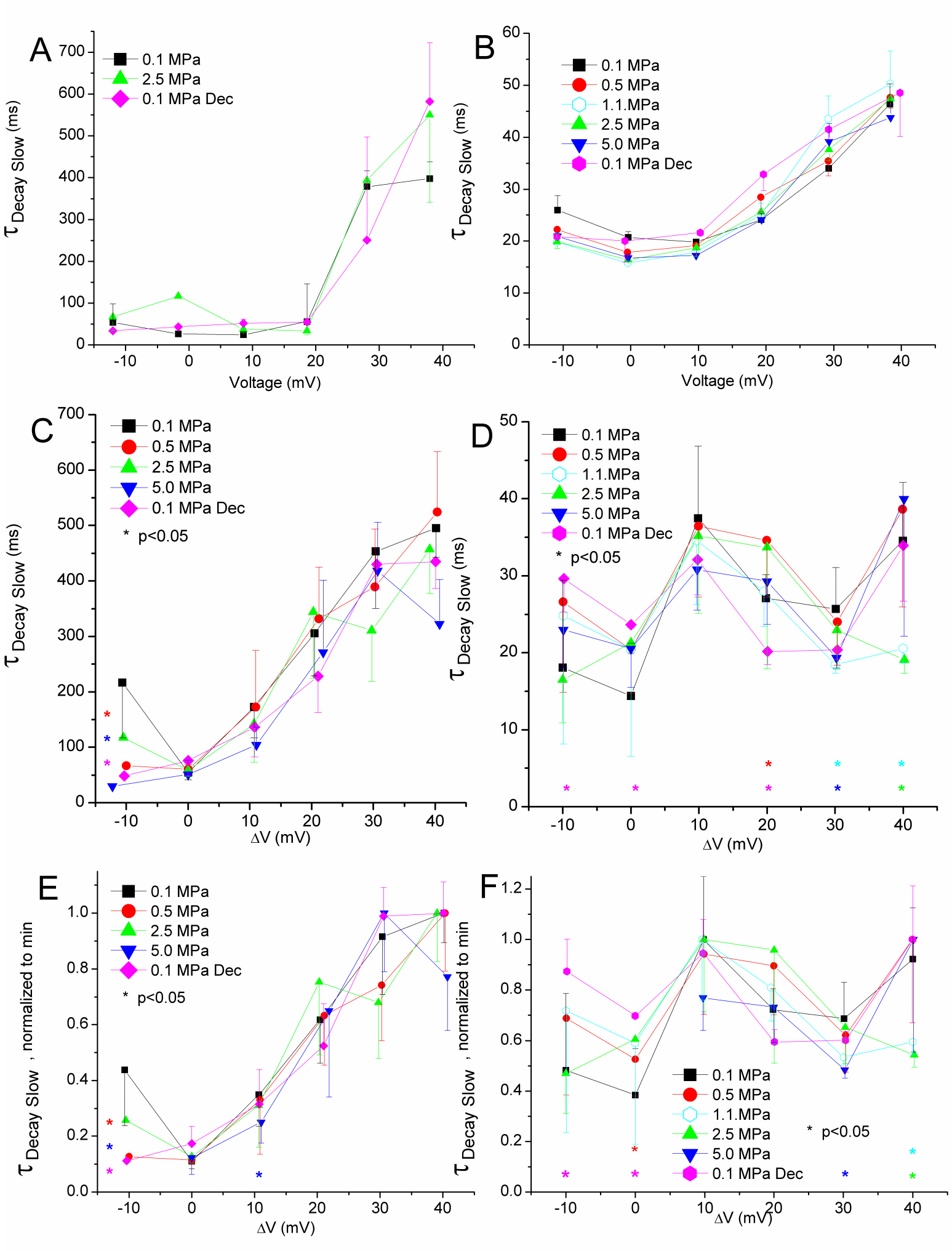
A
0.1 MPa
2.5 MPa
0.1 MPa Dec
τ Decay Slow (ms)
Voltage (mV)
B
0.1 MPa
0.5 MPa
1.1.MPa
2.5 MPa
5.0 MPa
0.1 MPa Dec
τ Decay Slow (ms)
Voltage (mV)
C
0.1 MPa
0.5 MPa
2.5 MPa
5.0 MPa
0.1 MPa Dec
* p<0.05
τ Decay Slow (ms)
ΔV (mV)
D
0.1 MPa
0.5 MPa
1.1.MPa
2.5 MPa
5.0 MPa
0.1 MPa Dec
* p<0.05
τ Decay Slow (ms)
ΔV (mV)
E
0.1 MPa
0.5 MPa
2.5 MPa
5.0 MPa
0.1 MPa Dec
* p<0.05
τ Decay Slow , normalized to min
ΔV (mV)
F
0.1 MPa
0.5 MPa
1.1.MPa
2.5 MPa
5.0 MPa
0.1 MPa Dec
* p<0.05
τ Decay Slow , normalized to min
ΔV (mV)

Figure 9.TIF

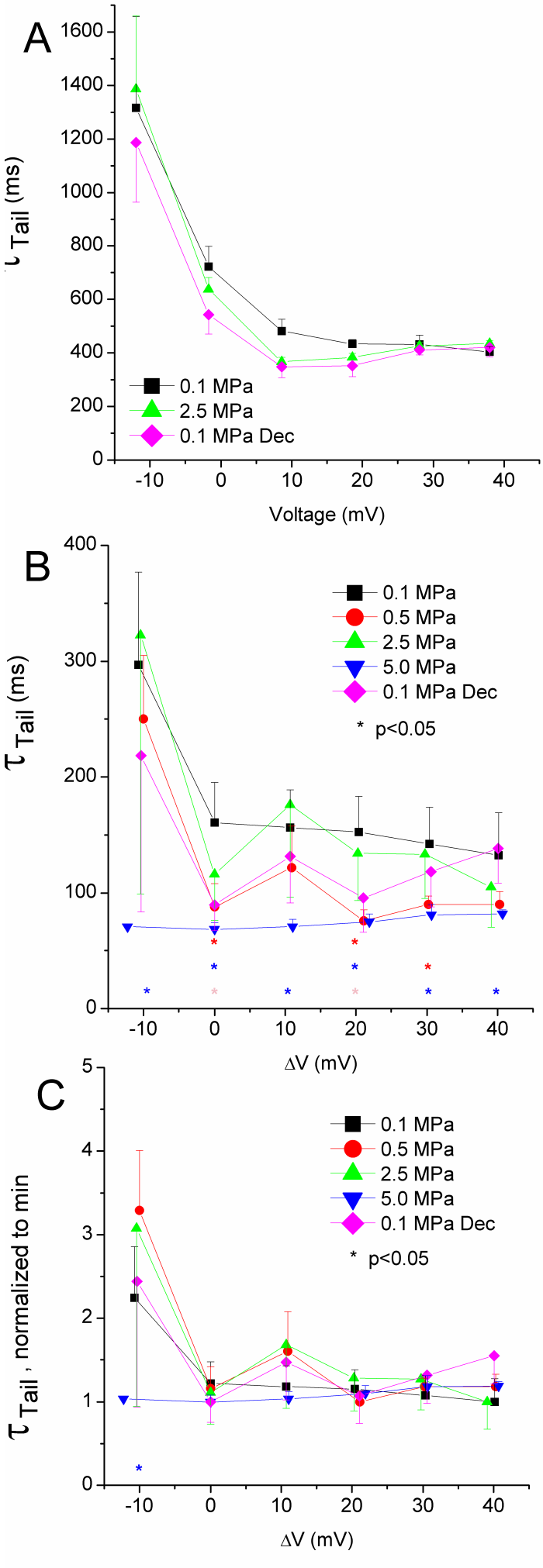
A
τ Tail (ms)
Voltage (mV)
0.1 MPa
2.5 MPa
0.1 MPa Dec
B
τ Tail (ms)
ΔV (mV)
0.1 MPa
0.5 MPa
2.5 MPa
5.0 MPa
0.1 MPa Dec
* p<0.05
C
τ Tail , normalized to min
ΔV (mV)
0.1 MPa
0.5 MPa
2.5 MPa
5.0 MPa
0.1 MPa Dec
* p<0.05